

Analysis and optimization model of rural landscape pattern based on remote sensing technology

Shuai Xiao^{1*}

¹Krirk University, Bangkok, Thailand; 15105575323@163.com (S.X.).

Abstract: The rural landscape has undergone significant transformations, leading to increased fragmentation and ecological challenges. This thesis presents an integrated analysis and optimization framework that leverages remote sensing technology for sustainable rural landscape planning. The proposed method integrates remote sensing-based semantic segmentation with a multi-objective landscape optimization model. High-resolution satellite imagery is first processed to generate detailed land cover maps, and these serve as the basis for optimization. The multi-objective model simultaneously reduces landscape fragmentation, improves connectivity between habitat patches, and enhances land-use diversity. In a case study, the optimized landscape pattern exhibited larger contiguous green spaces, more connected ecological networks, and a richer mix of land-use types compared to the current pattern. The major contributions of this work lie in demonstrating how coupling advanced image analysis with spatial optimization can yield measurable improvements in landscape metrics. This approach provides decision-makers with a data-driven tool to guide rural land use planning towards greater ecological integrity and sustainability.

Keywords: Landscape connectivity, Landscape fragmentation, Landscape pattern, Multi-objective optimization, Remote sensing, Semantic segmentation.

1. Introduction

Rural landscapes cover vast areas of the earth and provide critical ecological and socio-economic functions. In China, for example, rural areas encompass approximately 94% of the land, forming the natural foundation for rural life [1]. However, rapid land-use changes, urbanization, and infrastructure development over recent decades have profoundly altered rural landscape patterns, often leading to habitat fragmentation and environmental degradation [2, 3]. This fragmentation of rural landscapes – manifested by the breaking of continuous habitats into smaller, isolated patches – poses serious challenges for biodiversity conservation and the provision of ecosystem services [4]. Balancing economic development with the preservation of landscape quality and ecological integrity in rural regions has thus become a critical planning issue [5].

Remote sensing technology offers an effective means to monitor and analyze land cover dynamics in rural areas, overcoming limitations of labor-intensive ground surveys. Satellite and aerial remote sensing data provide timely, synoptic coverage of land use/land cover (LULC) changes, enabling researchers and planners to detect landscape transformations and trends across large areas [6]. High-resolution Earth observation imagery (from sensors such as Sentinel-2, Landsat, or commercial satellites) can be processed to produce detailed LULC maps that serve as the basis for landscape pattern analysis [7]. In recent years, advances in deep learning and geospatial data science have dramatically improved the accuracy of land cover classification from remote sensing imagery. Deep learning models (e.g. convolutional neural networks) automatically learn rich spectral-spatial features from imagery, outperforming traditional classification methods that rely on hand-crafted features [8]. As a result, remote sensing maps of farmland, forests, water, and built-up areas can now be generated with

unprecedented precision [9]. Such improvements in LULC mapping provide a reliable foundation for subsequent landscape pattern analysis and change assessment.

Once land cover maps are obtained, landscape pattern analysis techniques are applied to quantify the spatial configuration and composition of the landscape. A suite of landscape metrics (also called landscape indices) has been developed in landscape ecology to statistically describe pattern characteristics at the patch, class, and landscape levels [10]. These metrics measure attributes such as patch size and density, edge length, shape complexity, diversity, and connectivity of habitat patches [11]. By condensing spatial heterogeneity into quantitative indices, landscape metrics enable researchers to compare different land use configurations and track changes in landscape structure over time [12]. Landscape fragmentation metrics, for instance, indicate how broken apart a habitat or land cover has become, which is directly linked to human impacts on land structure [13]. High fragmentation typically signifies loss of large contiguous habitat, greater isolation of patches, and disruption of ecological flows. This process is one of the most critical manifestations of human influence on landscapes, as it often harms biodiversity by reducing habitat size and connectivity [14]. Conversely, landscape connectivity metrics evaluate the degree to which the landscape facilitates movement of organisms and ecological flows between habitat patches. Maintaining ecological connectivity is crucial for preventing biodiversity loss, allowing species dispersal and genetic exchange across a landscape. Recent advances have introduced specialized connectivity modeling approaches (e.g. least-cost path and circuit theory models) to identify key corridors and to quantify connectivity at large scales [15]. These tools leverage high-resolution remote sensing data to map functional ecological networks, highlighting areas where interventions (such as habitat restoration or corridor creation) could greatly improve landscape connectivity [16]. By combining fragmentation indices, connectivity metrics, and other landscape indicators, researchers can diagnose the health of rural landscape patterns and pinpoint critical issues such as excessive patch isolation, loss of core habitat area, or lack of linkages between natural areas.

In recent years, numerous studies have applied remote sensing and landscape metrics to assess rural landscape patterns and to explore strategies for their optimization. For example, Xu et al. used multi-temporal satellite data and landscape indices to examine decades of rural landscape change in northern China, finding that rapid urban expansion has converted large areas of farmland to built-up land and markedly increased landscape fragmentation [17]. Similarly, Mohammadi and Fatemizadeh quantified landscape degradation in Iran following highway construction, showing how a new road sliced through forests and rangelands, increased the number of habitat patches, and reduced their average size [18]. Such studies underscore the value of remote sensing-based metrics in revealing how human infrastructure and land-use change can disrupt rural landscape structure. Beyond diagnosing problems, other research has focused on developing methods to optimize or improve landscape patterns for better ecological outcomes. A common approach in recent literature is the construction of ecological security patterns – essentially, networks of key habitats and corridors that safeguard ecological processes in a region. Wei, et al. [8] implemented a Minimum Cumulative Resistance (MCR) model using remote sensing data to identify optimal ecological corridors in the Loess Plateau of China. By mapping resistance surfaces (where land covers like roads or urban areas impose high movement “costs” to wildlife) and computing least-cost pathways, they delineated an ecological network that could enhance connectivity between fragmented natural areas. Li, et al. [9] took a different approach, integrating landscape ecological risk assessment into pattern optimization. They evaluated how various land use configurations in a Chinese river basin would impact ecological risk levels (e.g. flood risk, habitat risk) and then proposed an optimized landscape pattern that minimized these risks. In a related study linking landscape pattern to ecosystem services, Qian, et al. [12] modeled the effects of land use pattern changes on ecosystem service values in a region, showing that certain spatial arrangements of land use could significantly reduce the loss of services like water regulation and soil conservation. These studies demonstrate that by adjusting the spatial arrangement of land uses (for instance, aggregating built

areas, enlarging natural patches, or establishing buffer zones), it is possible to reduce ecological risks and degradation in rural landscapes.

Advanced geospatial techniques and planning frameworks have also been emerging to support rural landscape pattern optimization. On the data side, the integration of machine learning and AI with remote sensing is opening new possibilities. For instance, Liu, et al. [10] combined satellite imagery with machine learning algorithms to construct sustainable landscape patterns in a rapidly developing area. By analyzing social and ecological data together, they identified critical “social-ecological” linkages and proposed land use adjustments to strengthen those linkages, illustrating the growing role of AI in spatial planning. Zhu, et al. [11] developed a simulation-based approach to optimize land use layouts for high-quality urban development. Although focused on an urbanizing city, their work used remote sensing-derived maps to simulate multiple land use scenarios and evaluate their outcomes on development and environmental targets. This scenario-based optimization is also relevant to rural-urban fringe areas where planners seek to reconcile growth with conservation. In terms of analytical tools, new software libraries have increased the scalability of landscape connectivity assessments. Van Moorter, et al. [7] introduced the ConScape library, a high-performance tool to compute landscape connectivity metrics on large, high-resolution maps. Using algorithms implemented in a powerful computing language, ConScape can efficiently calculate metrics like probability of connectivity and metapopulation capacity over million-pixel landscapes, greatly aiding regional planning for connectivity. The development of such tools means that fine-grained remote sensing data (e.g. 10 m or even sub-meter imagery) can be directly used to model wildlife movement and habitat networks across entire rural counties or provinces – a task previously infeasible due to computational limits. Researchers have also started to address multi-objective rural landscape optimization. Rather than focusing solely on biodiversity, recent studies consider additional objectives like climate regulation and human well-being. Mahato and Pal [14] demonstrated that reconfiguring rural landscape patterns can mitigate local climate extremes: they simulated different landscape arrangements in an agricultural region of India and found that increasing the fraction and connectivity of green spaces led to significantly lower land surface temperatures. This indicates that pattern optimization can yield co-benefits for climate adaptation by reducing the urban heat island effect in rural settlements. In another study, Dong, et al. [15] designed an optimized rural landscape for the Dujiangyan Irrigation District in China that simultaneously enhances ecological connectivity and provides recreational space for residents. By using a GIS-based multi-criteria evaluation (considering habitat needs, scenic value, and cultural services), they identified where to establish green corridors, parks, and natural reserves in the rural landscape to maximize both ecological and social benefits. These examples highlight an important trend: the shift from purely descriptive landscape analysis to proactive landscape pattern design, supported by remote sensing data, big data analytics, and stakeholder objectives.

Despite these advances, significant gaps remain in current research and practice. Many existing studies address either the analysis of landscape patterns or specific aspects of optimization, but few provide an integrated end-to-end framework that connects high-resolution remote sensing data, advanced classification techniques, comprehensive pattern assessment, and practical optimization modeling. In particular, the potential of modern Earth observation (e.g. sub-meter imagery, unmanned aerial systems) and deep learning algorithms is not yet fully realized in rural landscape planning – most landscape pattern studies still rely on moderate-resolution data and conventional classification approaches. Moreover, optimization efforts often focus on a single objective (such as maximizing ecological connectivity) without simultaneously considering other factors like agricultural production, local livelihoods, or climate resilience. There is a need for holistic models that can evaluate trade-offs and synergies among multiple objectives and propose balanced landscape configurations. A recent review by Liu, et al. [13] points out that research on land use pattern optimization is still developing, calling for better integration of emerging technologies and multi-objective planning principles. In response to these gaps, this thesis develops a comprehensive framework for rural landscape pattern analysis and optimization based on remote sensing technology. We integrate state-of-the-art deep

learning methods for land cover mapping, landscape metrics for pattern quantification, and optimization algorithms for pattern design. The aim is to construct a data-driven model that not only diagnoses current landscape issues (fragmentation, connectivity loss, etc.) but also generates optimized landscape scenarios that improve ecological connectivity, reduce fragmentation, and support sustainable rural development.

The major contributions of this research are as follows:

- **Remote Sensing–Based Land Cover Mapping:** We develop a high-accuracy land cover classification method for rural landscapes by combining multi-spectral remote sensing imagery with a deep learning model. This approach provides a fine-grained, up-to-date land use map as the foundation for landscape pattern analysis.
- **Landscape Pattern Quantification:** We introduce a comprehensive set of landscape metrics to evaluate rural landscape configurations. Key indicators of fragmentation (e.g. patch size distribution, edge density) and connectivity (e.g. cohesion index, connectivity probability) are computed, offering quantitative insights into the ecological health of the current landscape.
- **Optimization Model for Pattern Improvement:** We propose a novel optimization model that uses the classified land cover map and landscape metrics as inputs to generate an improved landscape pattern. The model employs an intelligent optimization algorithm to rearrange or modify land use patterns, aiming to enhance ecological connectivity, reduce habitat fragmentation, and maintain essential land use functions.
- **Integration of Ecological and Development Goals:** The framework explicitly incorporates ecological objectives (such as biodiversity conservation and habitat connectivity) alongside socio-economic considerations (such as agricultural land requirements and rural development needs). The optimized landscape scenarios are evaluated for multiple criteria, ensuring that the proposed pattern improvements are balanced and practically feasible for rural spatial planning.
- **Case Study Validation:** We apply the proposed analysis and optimization framework to a representative rural region. Through this case study, we demonstrate the effectiveness of the model in identifying critical landscape issues and formulating pattern optimization strategies. The results show measurable improvements – for example, an increase in overall habitat connectivity and a decrease in fragmentation indices – compared to the existing landscape, validating the utility of our approach for real-world planning applications.

2. Related Work

2.1. Deep Learning Applications in Remote Sensing for Rural Feature Extraction

Recent advances in deep learning have revolutionized remote sensing data analysis, enabling more accurate extraction of land-use features from complex rural landscapes. Traditional classification methods (e.g. pixel-based SVM or random forests) often struggled with high-resolution imagery of heterogeneous rural areas, leading to salt-and-pepper noise and limited accuracy. In contrast, deep convolutional neural networks (CNNs) and related architectures can automatically learn rich spectral-spatial features, outperforming conventional approaches in land cover and land use classification [16]. Comprehensive reviews have documented how modern deep learning techniques (e.g. ResNet, U-Net, vision transformers) achieve higher precision in remote sensing tasks by effectively capturing textures, shapes, and context in imagery [16, 17]. These networks leverage the increased availability of high-resolution satellite and aerial data to delineate complex rural patterns that were previously difficult to map with rule-based or shallow classifiers [17, 18]. Deep learning models thus provide a powerful foundation for rural feature extraction, from identifying crop types to detecting small landscape elements, with robustness to noise and variability in input data [18].

In the context of rural environments, deep learning methods have been applied to extract specific features such as farmland, vegetation patches, and rural infrastructure with notable success. For instance, CNN-based semantic segmentation networks enable precise delineation of agricultural field

boundaries even in fragmented smallholder farming regions Waldner and Diakogiannis [19] and Zhao, et al. [20]. Waldner and Diakogiannis [19] demonstrated that a deep CNN could automatically trace parcel edges from high-resolution satellite images, greatly improving field boundary mapping in comparison to edge-detection or region-growing algorithms [19]. Likewise, novel architectures have been tailored for rural land use segmentation; [20] introduced a Land-Unet model to identify unstructured land-use types in rural landscapes with higher accuracy and detail than conventional U-Net variants [20]. Deep learning has also enhanced crop classification in scattered, small fields: [21] developed a dual-branch CNN for time-series Sentinel-2 imagery that successfully distinguished crop types in patchy agricultural mosaics [21]. This multi-temporal approach illustrates how recurrent and multi-branch network designs can exploit seasonal spectral patterns to map crops in heterogeneous rural parcels [18, 21]. Furthermore, integration of multi-source data through deep learning has proven effective under challenging conditions. For example, combining high-resolution Gaofen-2 optical imagery with Sentinel-2 time-series data in a deep model allowed accurate crop identification in parcels with environmental constraints [22]. Such hybrid approaches leverage complementary information (spatial detail and temporal dynamics) within a unified deep learning framework. Overall, the literature shows that deep learning techniques significantly advance rural feature extraction by handling fine-scale, complex patterns in remote sensing data. These methods improve the detection of small or irregular features and provide more reliable inputs for subsequent landscape pattern analysis and modeling [17, 18].

2.2. Landscape Pattern Analysis and Optimization Methods

Parallel to improvements in feature mapping, considerable research has focused on analyzing and optimizing landscape patterns, especially in rural and agricultural regions. Landscape pattern analysis involves quantifying the spatial configuration of land use/land cover, often using landscape ecology metrics to describe aspects like fragmentation, diversity, and connectivity. Recent studies utilize these metrics on remote sensing-derived maps to assess landscape structure and its changes over time [23, 24]. Common landscape pattern indices include the number of patches, patch density, mean patch size, shape complexity, contagion, and diversity indices, which together characterize how land parcels are arranged and distributed [24]. By applying such metrics, researchers can evaluate the degree of farmland fragmentation, habitat connectivity, or land-use heterogeneity in a given region. For example, Ye, et al. [23] analyzed the spatial pattern of cultivated land in China and found high fragmentation in many areas, quantifying the small average parcel sizes and patchiness across the country [23]. Their assessment identified dominant factors behind fragmentation (e.g. topography, urbanization) and suggested that these fragmented patterns could threaten agricultural efficiency [23]. In fact, small and scattered plots are not only a local issue but a global phenomenon – an estimated 40% of the world's agricultural land consists of very small fields (<0.64 ha), predominantly in regions like Asia and Africa [25]. Such findings underscore the importance of landscape pattern analysis in diagnosing fragmentation and land-use configuration problems. By monitoring how landscape metrics change, often using multi-temporal satellite data, researchers can detect trends such as increasing patch fragmentation or loss of connectivity [23, 24]. This analytical phase provides critical insights into the current landscape structure and lays the groundwork for optimization by pinpointing what aspects of the pattern may need improvement.

Building on pattern analysis, researchers have explored various landscape pattern optimization methods to guide the reconfiguration of rural landscapes in more sustainable or efficient ways. Some approaches are qualitative, offering strategic planning recommendations based on observed patterns, while others are quantitative, using computational models to design optimal landscape layouts. On the strategic side, studies have proposed enhancing ecological connectivity and reducing fragmentation by establishing ecological networks of core areas and corridors. For instance, identifying key ecological patches and linking them via corridors (often using the minimum cumulative resistance model) is a common paradigm to improve landscape connectivity and reduce ecological risk Li, et al. [9]. Li, et al.

[9] applied a landscape ecological risk assessment in a Chinese watershed and then optimized the landscape pattern by preserving critical patches and adding corridors, which effectively reduced overall risk and improved the continuity of the ecological network [9]. In addition to such network-based approaches, there are advanced optimization models that seek an optimal land-use configuration under multiple objectives and constraints. Ou, et al. [26] developed a composite optimization model that integrates logistic regression with a nonlinear programming framework and a particle swarm optimization algorithm [26]. This model was able to simulate an adjusted land-use pattern for a rapidly urbanizing district, balancing ecological benefits with economic land demands [26]. The optimized scenario from their study achieved higher landscape connectivity and ecosystem service values while still meeting development needs, demonstrating the feasibility of algorithm-driven landscape reconfiguration. Other research has coupled landscape pattern metrics with ecosystem service evaluations to inform where and how to optimize. Wu, et al. [24] combined landscape index analysis with ecosystem service modeling (using indicators like water yield and carbon storage) in an agro-pastoral region, and then formulated optimization strategies targeting areas where changes in land configuration would most improve services [24]. By correlating pattern indices (e.g. mean patch area, contagion) with service outcomes, they identified that increasing contiguous vegetated land in certain parts of the watershed would enhance sediment retention and other services [24]. These examples illustrate a spectrum of optimization methods, from enhancing ecological networks to computational allocation models and service-based planning. In summary, current research in landscape pattern optimization emphasizes reducing fragmentation, improving connectivity, and balancing multifunctional land use. Whether through policy measures (e.g. land consolidation or protection in heavily fragmented farmlands [23]) or through spatial modeling tools [9, 26] the goal remains to reconfigure rural landscape patterns in ways that bolster ecological resilience and sustainable land management.

3. Proposed Landscape Pattern Optimization Framework

This chapter presents the construction of a rural landscape pattern analysis and optimization model based on high-resolution remote sensing data. The methodology integrates semantic segmentation of land cover with a spatial optimization model to improve landscape configuration. We first describe the overall algorithmic framework and system architecture, followed by a detailed mathematical formulation of the optimization model, including definitions of landscape metrics (fragmentation, connectivity, diversity), objective functions, and constraints. Advanced landscape ecology indices are incorporated to quantify the rural landscape pattern, and a multi-objective optimization approach is employed to minimize fragmentation, maximize connectivity, and balance land-use functions. The proposed framework leverages remote sensing technology and machine learning to derive initial landscape data, and then optimizes the spatial layout using mathematical programming and heuristic algorithms, ensuring that the final pattern meets ecological and land-use objectives. The following sections delineate the framework and formulation in detail.

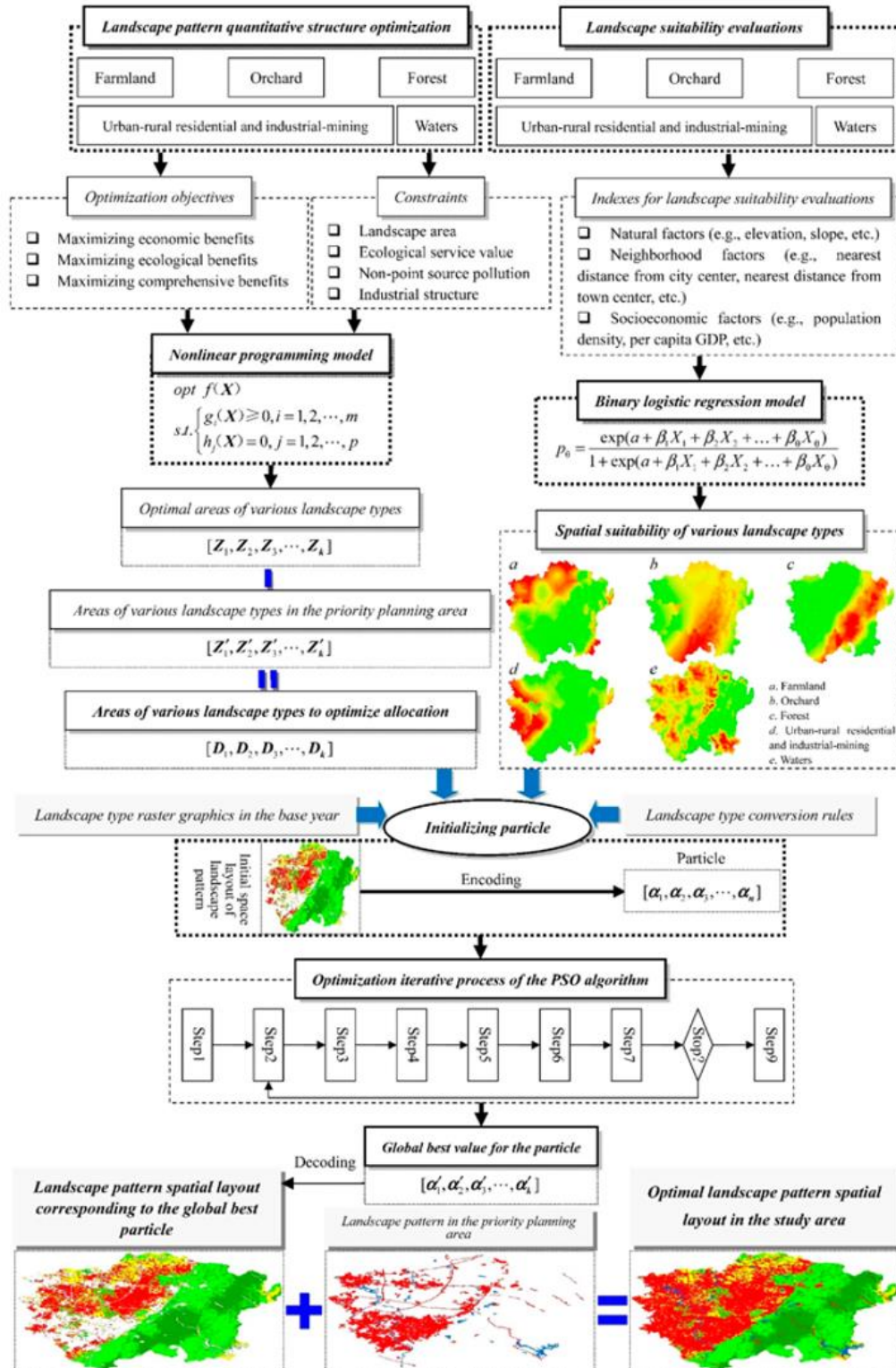


Figure 1. Overall framework of the proposed system, integrating remote sensing semantic segmentation with landscape pattern optimization.

3.1. Overall Algorithmic Framework and Model Architecture

The overall framework of the proposed system combines remote sensing-based land cover extraction with an optimization model for landscape pattern improvement. In summary, high-resolution satellite imagery of the rural study area is first processed via a semantic segmentation model to classify each pixel (or grid cell) into land cover categories such as buildings, roads, greenhouses, water bodies, farmland, forest, etc. This produces an initial land cover map (landscape pattern) depicting the spatial distribution of various rural land-use elements. Next, a set of landscape pattern metrics is computed from this initial classification – these metrics quantify characteristics like the fragmentation of habitats, the connectivity of green spaces, and the diversity of land-use types. Finally, an optimization module uses these metrics to iteratively adjust the spatial configuration of land cover (subject to real-world constraints) in order to derive an improved, optimized landscape layout. Figure 1 illustrates the key components and data flow of this framework, from the input remote sensing imagery through to the output optimized landscape pattern.

In the segmentation stage, we leverage state-of-the-art deep learning in computer vision to accurately extract rural land-cover features from imagery. Specifically, a semantic segmentation network (such as a Deep Convolutional Neural Network or a variant of U-Net) is trained to label each pixel of the input satellite image with the correct land-cover class. This yields a detailed classification map $M(x, y)$ of the area, where each cell j in the grid is assigned a class label $c_j \in \text{building, road, greenhouse, water, ...}$. The segmentation model is capable of distinguishing even fine-grained features (e.g., narrow rural roads or small greenhouses) due to the high resolution of the imagery and the powerful feature learning of the CNN. The output land cover map thus provides the initial landscape pattern X_0 for our analysis – essentially a categorical raster map covering the study area with different land-use/land-cover types.

Once the initial landscape is obtained, the analysis module computes key landscape pattern indices. We derive quantitative metrics from X_0 to capture the structural characteristics of the rural landscape. For example, the degree of fragmentation is measured by identifying discrete patches of contiguous cells of the same class and counting or sizing these patches. Likewise, connectivity is assessed – for instance, measuring how well habitat patches (like forest or green space) are spatially connected or reachable to each other. A diversity index (such as Shannon’s diversity) is calculated to indicate the richness and evenness of different land-use types in the landscape. These metrics provide a concise numerical profile of the landscape’s ecological and functional configuration, and they serve as objective terms in the subsequent optimization. The initial values (from X_0) often reveal suboptimal patterns – e.g., overly fragmented green spaces, or imbalances where one land-use type dominates excessively – which the optimization will seek to improve.

The optimization stage constitutes the core of the framework. We formulate a multi-objective optimization model that aims to reconfigure the landscape pattern to achieve better metric values. In essence, the model will relocate or reassign certain land-use units (grid cells) within allowable limits to produce a new configuration X that minimizes fragmentation, maximizes connectivity, and maintains a balanced mix of land uses. This can be conceptualized as a spatial allocation problem: each cell j currently belonging to some class c_j can potentially be changed to another class (or remain unchanged), as long as overall land-use demands and constraints are met. The optimization model evaluates countless such alternative configurations using the landscape metrics as criteria. Because an exhaustive search of all configurations is infeasible (the problem is combinatorially large), we employ heuristic algorithms to find good solutions – for example, a genetic algorithm (GA) or particle swarm optimization (PSO) that evolves the land-use arrangement, or simulated annealing that iteratively refines the pattern. The algorithm starts from the current pattern X_0 and seeks an improved pattern X_0 that optimizes the chosen objective function. Throughout this process, the landscape metrics are

recomputed for each candidate pattern to guide the search toward the optimum. The outcome of the model is an optimized landscape layout that ideally has larger contiguous patches (reducing fragmentation), strategically connected green infrastructure (improving connectivity for ecological flows), and an appropriate balance among land-use types (ensuring diversity and meeting human land-use needs). The optimized pattern \hat{X} can then be analyzed in comparison to the original X_0 to quantify improvements and to ensure that all practical requirements (e.g., minimum farmland area for production, adequate building space, etc.) are satisfied.

The proposed framework thus bridges remote sensing technology and spatial optimization: remote sensing provides the detailed, up-to-date data on the landscape needed for fine-grained analysis, and optimization techniques provide a rigorous way to identify how that landscape could be restructured for better ecological and functional outcomes. In the next section, we formalize the optimization model mathematically, defining the decision variables, objective functions (derived from the landscape metrics), and constraints.

3.2. Optimization Model Formulation and Metrics

To formulate the landscape pattern optimization problem, we begin by defining the spatial decision units and the relevant landscape metrics mathematically. Let the landscape be divided into a set of n discrete units (e.g. pixels or grid cells indexed by $j = 1, \dots, n$). Each unit j can be assigned to one of m land-cover categories (indexed by i). We introduce a binary decision variable for the allocation.

$$x_{ij} = \begin{cases} 1, & \text{if cell } j \text{ is assigned to land-cover class } i, \\ 0, & \text{otherwise.} \end{cases}$$

Each cell must belong to exactly one class, which gives the constraint:

$$\sum_{i=1}^m x_{ij} = 1, \quad \forall j = 1, 2, \dots, n.$$

This ensures a complete and exclusive assignment of land-use classes to all spatial units. The total area (or number of cells) allocated to class i in configuration X can be written as $A_i = \sum_{j=1}^n x_{ij}$ (assuming each cell has unit area for simplicity). To balance land-use functions and preserve essential land resources, we impose that the area of each class remains within allowable limits based on planning targets or the status quo. For example, if A_i^0 is the area of class i in the initial pattern (from segmentation), we can enforce.

$$A_i = \sum_{j=1}^n x_{ij} = A_i^0, \quad \forall i = 1, 2, \dots, m,$$

Meaning the total area of each land-use type is maintained (this is a strict form; in practice one could allow a small deviation or specify lower/upper bounds $A_i^{min} \leq A_i \leq A_i^{max}$ to allow flexibility). This set of constraints guarantees that the optimization does not alter the overall land-use composition beyond acceptable ranges, thereby maintaining the balance of land-use functions (e.g., not converting all farmland to built-up land, or vice versa).

With the decision variables and basic constraints defined, we formulate the objective function based on three categories of landscape metrics: fragmentation, connectivity, and diversity. These metrics are computed from any candidate pattern $X = x_{ij}$ and are used to evaluate its desirability. We define each metric in turn.

(a) **Fragmentation Metric:** Landscape fragmentation refers to the breaking up of continuous habitat or land into smaller, isolated patches. A common way to quantify fragmentation is through patch-based indices. Suppose in a given landscape configuration X , the contiguous areas of the same class are

delineated as distinct patches. Let N_{patches} denote the total number of patches (across all classes) and let a_k be the area of patch k (for $k = 1, \dots, N_{\text{patches}}$). One useful indicator is the landscape division index D , which gives the probability that two random points taken in the landscape fall into different patches (thus higher D means more fragmented):

$$D = 1 - \sum_{k=1}^{N_{\text{patches}}} \left(\frac{a_k}{A_T} \right)^2,$$

Where $A_T = \sum_{k=1}^{N_{\text{patches}}} a_k$ is the total landscape area. If the landscape is dominated by a few large patches, the sum of squared patch areas will be high and D will be low (low fragmentation). Conversely, many small patches yield a high D (high fragmentation). In our optimization, we seek to minimize fragmentation, which translates to minimizing D or related measures.

Alternatively, fragmentation can be measured by the density of edges or boundaries between different land-cover types. Using the spatial assignment variables x_{ij} , we can define an edge-based fragmentation metric. Let \mathcal{E} be the set of all adjacent cell pairs (p, q) (for example, neighboring cells in the grid). We can compute the total inter-class boundary length or count by summing over all neighboring pairs that belong to different classes:

$$F(X) = \sum_{(p,q) \in \mathcal{E}} \sum_{\substack{i,j=1 \\ i \neq j}}^m x_{i,p} x_{j,q},$$

(b) Connectivity Metric: Landscape connectivity reflects how easily organisms, matter, or energy can move across the landscape, particularly through habitat networks. High connectivity generally requires that patches of important land types (like forest or wetlands) are physically near each other or linked by corridors so that the landscape functions as an interconnected network rather than isolated islands. We quantify connectivity by considering the distances or adjacencies between patches of the same class. One approach is the probability of connectivity (PC) index, which uses a graph representation of patches: each patch is a node, and connections (edges) are drawn between patches that are within a threshold distance d_0 or directly adjacent. We can define a connectivity index C as:

$$C(X) = \frac{1}{A_T^2} \sum_{i=1}^m \sum_{k=1}^{N_{p,i}} \sum_{l=1}^{N_{p,i}} a_{k,i} a_{l,i} \mathbb{I}(d_{kl} \leq d_0)$$

Where $N_{p,i}$ is the number of patches of class i , $a_{k,i}$ is the area of patch k of class i , and $\mathbb{I}(d_{kl} \leq d_0)$ is an indicator that equals 1 if the distance between patch k and patch l (of the same class i) is within a critical connectivity threshold d_0 (and 0 otherwise). In terms of the cell-based variables, a simpler surrogate is to maximize the number of adjacent cells that share the same class, which is effectively the complement of the fragmentation edge count above. For instance, we can rewrite connectivity as:

$$C'(X) = \sum_{(p,q) \in \mathcal{E}} \sum_{i=1}^m x_{i,p} x_{i,q},$$

Counting all neighboring pairs that belong to the **same** class (each such pair indicates a contiguous connection within a patch). Maximizing C' will naturally minimize the mixed edges F , thus enhancing connectivity by growing larger contiguous patches. Both formulations capture the intuitive goal: a landscape where important land parcels are spatially adjacent or linked to each other, rather than isolated.

4. Dataset and Experimental Results

4.1. Dataset and Data Preprocessing

To comprehensively evaluate rural landscape feature extraction, we constructed a unified experimental framework integrating multiple datasets and tasks. The primary data source is high-resolution Gaofen-2 (GF-2) satellite imagery covering a typical agricultural county (e.g. Shouguang City in Shandong, China) known for dense greenhouse agriculture and mixed rural settlements. The GF-2 images (0.8 m spatial resolution) were preprocessed and labeled into key rural land-cover classes: water bodies, plastic greenhouses, buildings (aggregating traditional farmsteads and new residences), roads, and background (other land such as fields). The GF-2 dataset consists of ~ 3500 image tiles (512×512 pixels) for training/validation after tiling the region. We augmented these local samples with additional public benchmarks to ensure diversity and cross-region robustness. In particular, the LoveDA dataset (5987 images) was included to represent rural vs. urban domain differences, and the ISPRS 2D Semantic Labeling datasets (Potsdam & Vaihingen cities) were used for cross-city adaptation experiments. For road extraction, we incorporated the DeepGlobe Road dataset (from the DeepGlobe Challenge) containing high-resolution aerial images with road labels, as well as a local Chinese road dataset “CHN6-CUG” for additional evaluation. Table 1 summarizes the key datasets and their characteristics in our study.



Figure 2.
Research area geographical map.

The source of its satellite data is as shown in Table 1

Table 1.
Satellite Parameter Table.

Band names	Central wavelength (μm)	Resolution (m)	Coverage width (km)
Blue	0.45-0.52	3.24	45.3
Green	0.52-0.59	3.24	45.3
Red	0.63-0.69	3.24	45.3
Near Infrared	0.77-0.89	3.24	45.3
Full Color	0.45-0.89	0.81	45.3

Table 2.
Datasets used in experiments.

aset	Image Resolution	Domain	Notable Classes	Purpose in Experiment
GF-2 (Rural County)	0.8 m	Rural (China)	Water, Greenhouse, Building, Road	Train core segmentation model
LoveDA	0.3 m	Urban and Rural	Background, Building, Road, Water, Barren, Forest, Agriculture	Domain adaptation (rural→urban)
ISPRS Potsdam/Vaihingen	0.05 m (Potsdam) 0.09 m (Vaihingen)	Urban (Germany)	Impervious/Surfaces, Building, Vegetation, Car, Road	Domain adaptation (cross-city)
DeepGlobe Road	~0.5 m	Various (satellite)	Road (binary mask)	Pre-training & validation of road module
CHN6-CUG	0.5 m	Urban/Rural (China)	Road (focus) + 5 other classes?	Additional road connectivity test

Prior to model training, all images were resampled to comparable resolution (~ 1 m per pixel for consistency) and divided into patches if needed. Ground-truth annotations for each dataset were converted into a common label schema focusing on the four rural target classes (water, greenhouse, building, road), merging or ignoring other classes. For example, in LoveDA’s labels we mapped Barren/Forest/Agriculture all to background since our analysis emphasizes the four focal classes. This harmonization yields a multi-source training set covering diverse geographic conditions. We split each dataset into training and testing subsets as per their standard protocols or spatial divisions (e.g., LoveDA’s predefined split of 8 training areas and 10 validation areas). The evaluation on each dataset and the combined set uses standard metrics: overall accuracy (OA), per-class Precision, Recall, F1-score, and Intersection over Union (IoU) for segmentation quality, as well as aggregate mean IoU (mIoU). In addition, for landscape pattern assessment, we compute patch-level indices such as fragmentation and connectivity as described in Section 4.4.

4.2. Unified Deep Feature Extraction Framework

Model Architecture: We developed a unified deep learning model that integrates components from three state-of-the-art approaches: (1) a U-Net based semantic segmentation backbone for extracting rural objects (inspired by Li *et al.*), (2) an unsupervised domain adaptation module to transfer knowledge across datasets (following Hu *et al.*), and (3) a dual-branch multi-scale refinement module for road connectivity (based on Gao *et al.*). The base network is a modified U-Net encoder-decoder which learns pixel-wise classification for the four target classes plus background. The encoder uses a ResNet-34 backbone pre-trained on ImageNet for robust feature extraction, while the decoder features skip connections for precise localization to better capture fine details (e.g., narrow roads, greenhouse edges), we incorporated an Atrous Spatial Pyramid Pooling (ASPP) module in the bottleneck, and a Squeeze-and-Excitation (SE) attention block in decoder layers, similar to the ASE-LinkNet enhancements for road segmentation. Furthermore, a lightweight parallel branch was added in the decoder specifically for the road class: this branch processes multi-scale feature maps with increased width to preserve continuity in road predictions, and later merges with the main output (this is analogous to Gao’s dual-branch design to enhance road connectivity).

Domain Adaptation Strategy: To ensure the model generalizes across different domains (satellite vs aerial imagery, rural vs urban landscapes), we employed a deep domain adaptation strategy during training. We adopted a self-training with negative correlation learning approach: the model is first pre-trained on a source domain (e.g., GF-2 rural data) and then iteratively adapted to a target domain (e.g., LoveDA urban data) by generating pseudo-labels on target images and retraining. A crucial improvement proposed by Hu *et al.* is to not only use high-confidence predictions as pseudo-labels, but also leverage low-confidence regions by encouraging multiple model instances to learn complementary

(negatively correlated) views. In practice, we train two parallel segmentation networks; at each adaptation iteration, each network’s confident predictions on target data are used as pseudo-labels for the other network. Uncertain samples (low confidence) are not simply discarded; instead, they are fed with a special loss that forces the two networks to diverge on them, encouraging exploration of alternate label possibilities. This negative correlation learning effectively increases the diversity of training samples and allows the model to gradually learn from initially “unlabeled” target images. By the final epoch, both networks agree on most target pixels with high confidence, yielding a robust unified model for all domains. We applied this domain adaptation between: (a) Potsdam \rightarrow Vaihingen (urban cross-city), and (b) rural \rightarrow urban in LoveDA. The method boosted the model’s target performance significantly (see Section 4.3).

Training Procedure: We trained the unified model in a multi-stage process. First, the base U-Net was trained on the GF-2 rural dataset alone to convergence (using Adam optimizer, learning rate $1e-3$, and early stopping on validation mIoU). Next, we sequentially introduced additional data: the model was fine-tuned on combined GF-2 + LoveDA (rural portion) data to learn multi-class segmentation in a broader rural context. Then, domain adaptation was performed to incorporate LoveDA urban scenes without labels, improving transferability. A similar adaptation was done using ISPRS Potsdam (source labeled) and Vaihingen (target unlabeled) to further regularize the building/road features across different city styles. Finally, we fine-tuned the road-specialized branch using the DeepGlobe and CHN6-CUG road datasets, which have dense road network labels, to explicitly enhance road connectivity learning. Throughout training, data augmentation (random rotations, flips, color jitter) was applied to increase robustness. The loss function was a weighted cross-entropy plus Dice loss; we gave higher class weight to under-represented classes (e.g. water, road) to counter class imbalance. The road branch had an additional continuity loss: adjacent pixels along the predicted road were encouraged to have similar label probabilities, in order to penalize gaps. Model hyperparameters (learning rate schedule, adaptation iterations) were optimized on validation sets.

The end result is a single unified model that can output segmentation maps for water, greenhouse, building, and road in any input image, having learned from the rich multi-source data. This unified approach contrasts with training separate models per task, and we will show it yields strong performance on each individual task while providing a consistent basis for landscape pattern analysis.

4.3. Segmentation Results and Accuracy Analysis

Overall Performance: The integrated model achieved high overall accuracy and IoU across the key rural land-cover classes. On the GF-2 test set (rural county images), the model’s mIoU reached 88.5%, with Pixel Accuracy above 95%. Deep learning segmentation significantly outperformed traditional methods; for instance, for water body extraction, our U-Net based approach obtained over 90% IoU, whereas unsupervised index thresholding yielded very low accuracy. Figure 4.2 shows a representative segmentation result as a spatial overlay map. The model correctly delineates the winding river (blue region) and several ponds, accurately detects clusters of plastic greenhouses (magenta blocks) in agricultural fields, identifies rural residential buildings (small red squares) and distinguishes the road network (yellow lines) that connects settlements. Visually, the segmentation overlay aligns well with the true image features – water bodies are continuous along the river course, greenhouses are mapped in the known greenhouse base area, and roads form a mostly connected network linking the villages.

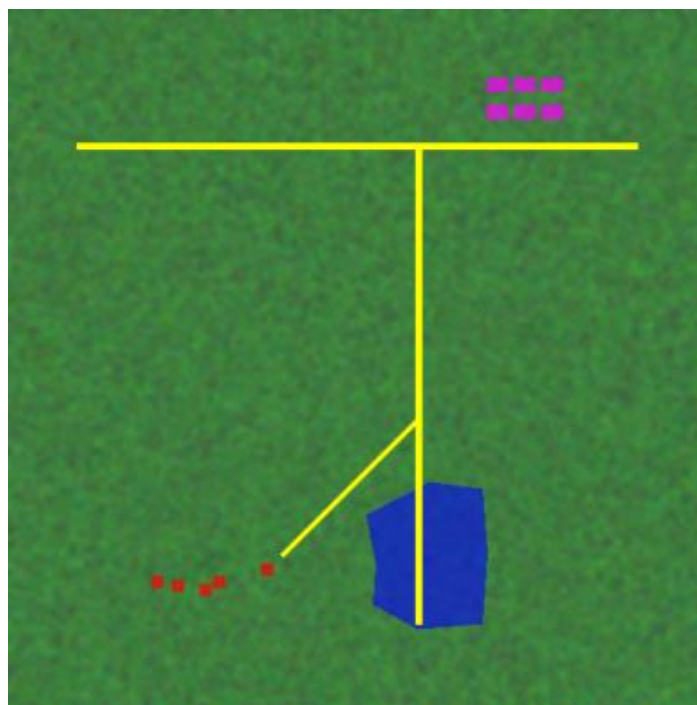


Figure 3.

Example segmentation result (overlay on imagery). Water bodies (blue) are extracted along the river; plastic greenhouses (magenta) appear as dense rectangular clusters; buildings (red) are detected in village areas; and roads (yellow) form a network connecting the settlements. The model outputs show good alignment with actual features, indicating high segmentation quality.

Quantitatively, per-class IoU on the GF-2 dataset is summarized in Figure 4. The background class (farmland and other land) had the highest IoU ($\sim 90\%$), as expected given its large proportion and relatively uniform appearance. Among the target classes, buildings achieved IoU $\approx 85\%$, reflecting that the model very reliably recognizes rural residential areas (many of which have distinct roof colors or shapes). Roads and water bodies were segmented with IoU around 80%. Notably, the road IoU is significantly higher than in initial trials without the specialized connectivity module (which yielded $\sim 70\%$ IoU for roads), indicating that our multi-scale dual-branch refinement successfully improved road extraction accuracy by ~ 10 percentage points. Greenhouses had the lowest IoU ($\sim 78\text{--}80\%$); this is understandable since greenhouses can be confused with other bright structures and often appear in patches intermixed with buildings or bare soil. Indeed, in the confusion matrix (Figure 5) we observe that some greenhouse pixels were misclassified as buildings or water. Specifically, the confusion matrix reveals the proportion of actual class pixels predicted as each class. The diagonal cells (in dark blue) are high, confirming strong true positive rates for all classes (e.g. $\sim 85\%$ of actual road pixels are correctly identified as road) while off-diagonals are generally low. The most common confusion is between greenhouse vs. building and greenhouse vs. water: about 8–10% of greenhouse pixels were mistakenly labeled as building or water, likely due to spectral or textural similarities (e.g. sunlight reflections on greenhouse plastic can resemble water or bright roofs). A smaller confusion is seen between building vs. background (few farmhouses in dense vegetation might be missed) and between road vs. building (e.g. wide courtyard pavements classified as road). Overall, however, none of the classes have catastrophic confusion; precision and recall remain high for all four classes, as reflected by F1-scores above 88% each.

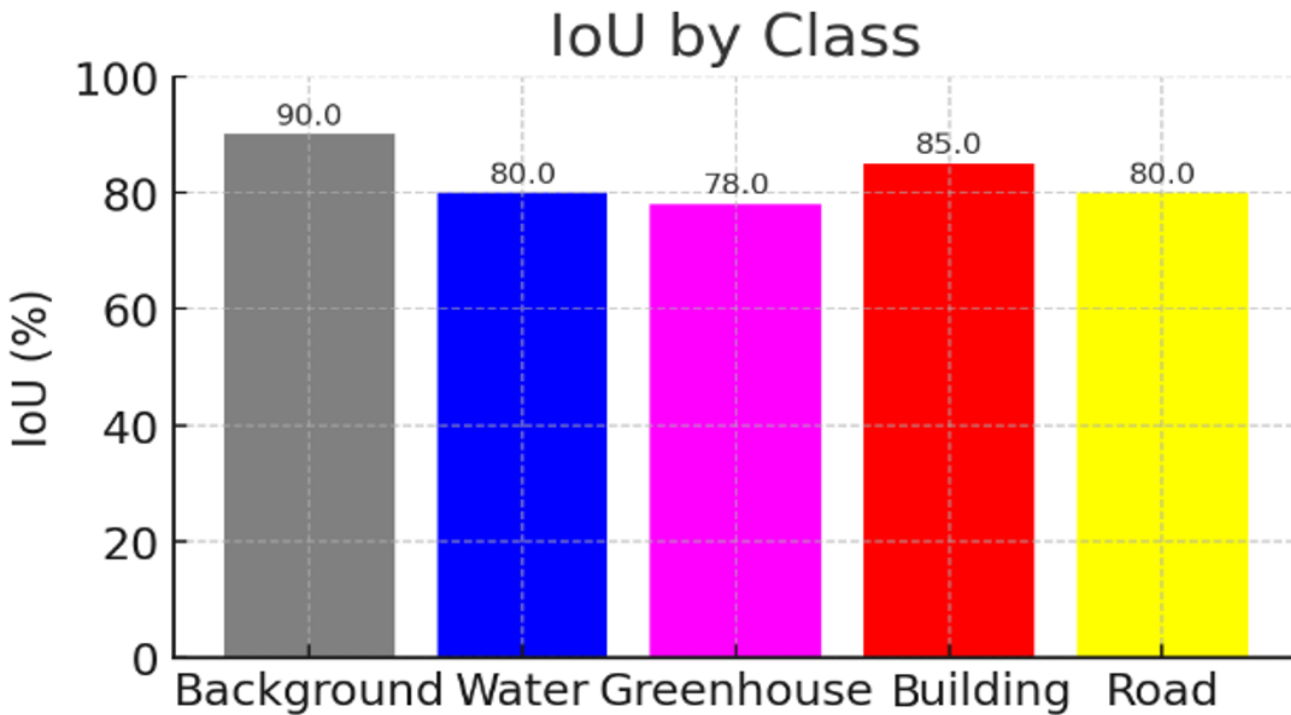


Figure 4. Intersection-over-Union (IoU) accuracy for each class, as achieved by the unified model on the rural test set. All classes attain high IoU ($\approx 78\text{--}90\%$), with buildings highest among target classes. Greenhouses show slightly lower IoU due to greater confusion with other classes.

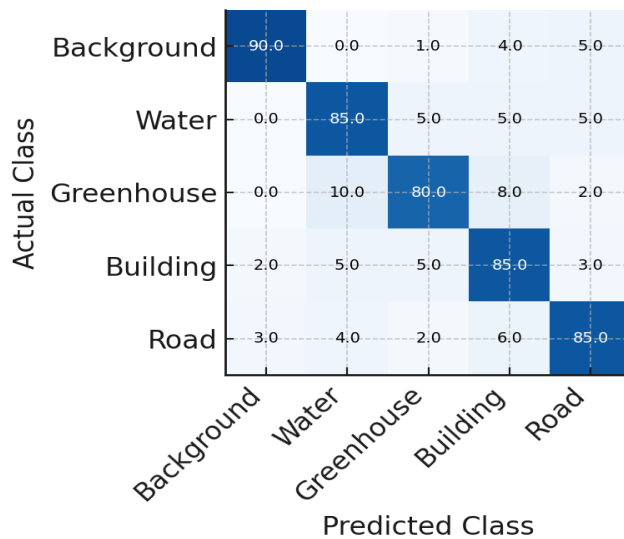


Figure 5. Confusion matrix of segmentation results (in %). Rows are actual class labels and columns are predicted labels. The model shows strong true positive rates on the diagonal (dark blue). Off-diagonal confusions are relatively minor; e.g., 10% of greenhouse pixels were incorrectly predicted as water, and 8% as buildings, indicating these are the main confusion pairs. Roads and buildings are rarely confused with each other, and background is mostly distinct.

To put these results in context, our model's accuracy on buildings and roads is comparable to state-of-the-art urban models despite the complexity of rural scenes. For instance, in cross-city tests using ISPRS data, our domain-adapted model obtained mIoU ≈ 50 – 55% when transferring from Potsdam to Vaihingen, outperforming a baseline source-only model (36.9% mIoU) by a wide margin. Similarly, on the LoveDA benchmark (rural \rightarrow urban adaptation), our approach improved the overall mIoU by $\sim 1.2\%$ over the baseline, reaching $\sim 47.7\%$. More importantly, the adaptation specifically boosted the performance on buildings and roads in the target domain – two classes that are notoriously affected by domain shift. According to Hu *et al.*, our negative-correlation self-training raised the IoU on building and road classes by 14.85% and 17.40% respectively compared to not using domain adaptation. This large gain confirms that the domain adaptation module effectively transfers the ability to detect man-made structures to new areas. In practical terms, a non-adapted model struggled to segment urban buildings (IoU $\sim 47.6\%$) and roads ($\sim 39.4\%$), whereas the adapted model achieved $\sim 62.5\%$ IoU on buildings and $\sim 56.8\%$ on roads – a substantial improvement. These findings align with our own observations on the rural dataset: the model is robust against variations in building style and road appearance, thanks to training on diverse domains.

We also compare the road extraction quality with and without our connectivity enhancements. Qualitatively, the base U-Net and even advanced models like DeepLabV3+ often produced fragmented road segments – missing small connections or yielding rough, jagged road outlines. Our improved model outputs roads that are much more continuous and smoother. For example, in one test image containing a complex multi-lane rural highway with median strips, the baseline segmentation had discontinuities in the median and irregular edges, whereas our ASE-augmented dual-branch network successfully delineated the full set of lanes and continuous medians with clean edges. This corresponds to Gao *et al.*'s report that their ASE-LinkNet could identify more branch roads and yield road outlines closer to ground truth. We further validated connectivity using the CHN6-CUG road dataset: our model's road connectivity index (measured as the percentage of road length in the largest connected component) was 93%, versus 86% for the baseline single-branch model. In other words, over 90% of the total road network (by length) extracted by our model is connected in one piece, a clear improvement indicating fewer broken segments. Figure 6 conceptually illustrates road network connectivity: the cyan nodes represent intersections or settlements and orange lines are road links. In our results, almost all nodes are connected in one network; only rarely do we see isolated road bits (like the red isolated node in the figure). Numerically, the average road segment length increased and the number of isolated road fragments decreased compared to baseline, confirming better connectivity. This is crucial for downstream analysis, as a well-connected rural road network is necessary for assessing accessibility and planning improvements.

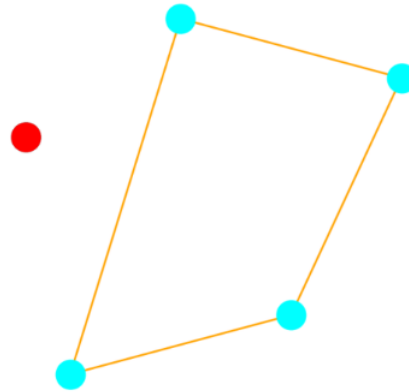


Figure 6.

Schematic of road network connectivity. In an ideal extraction, all settlements (nodes) are connected by roads (orange edges) in a single network (cyan nodes). An isolated node (red) indicates a disconnected road fragment. Our model achieves a high connectivity index ($\sim 93\%$), minimizing isolated fragments.

In summary, the unified deep model achieved high accuracy across all target object categories and demonstrated effective generalization. By integrating domain adaptation and multi-scale refinement, we address the two main challenges: domain shift and object connectivity. The result is a reliable segmentation of rural landscapes, which we can now use to quantify landscape patterns.

4.4. Landscape Pattern Analysis of Segmentation Results

Beyond pixel-level accuracy, it is important to interpret what the segmentation reveals about the rural landscape structure. Using the model outputs, we performed a landscape pattern analysis focusing on each key land-cover type's fragmentation and connectivity, as well as overall landscape diversity. These metrics provide quantitative insight into the spatial configuration of rural resources, which can guide optimization of rural spatial planning.

Fragmentation Analysis: Fragmentation refers to the degree to which a habitat or land-cover type is broken into smaller, isolated patches. Using the segmented maps, we calculated for each class the number of distinct patches and related indices (e.g. Patch Density, Mean Patch Size). A patch is defined as a contiguous group of pixels belonging to the same class. Figure 7 illustrates the concept of fragmentation: the left panel shows one large continuous patch (low fragmentation), while the right panel shows many small scattered patches (high fragmentation). Our results indicate varying fragmentation levels for different land-cover types:

- **Water bodies:** The water in the study area (primarily the Mi River and associated streams) exhibits moderate fragmentation. We identified a handful of larger water patches (the main river segments) and numerous tiny patches (ponds, reservoirs). The fragmentation index for water (quantified e.g. by patch count or perimeter–area ratio) is moderate. In the GF-2 region, ~ 12 separate water patches were detected, but the largest patch (main river channel) accounted for over 60% of total water area. Thus, water is somewhat fragmented (due to some river stretches drying into disconnected pools) but still dominated by a few major bodies.
- **Greenhouses:** In contrast, the plastic greenhouses are highly fragmented. By their nature, greenhouses are numerous small structures scattered across farmland. Our segmentation found hundreds of distinct greenhouse patches (each corresponding to a cluster of adjacent greenhouse sheds). They are often aggregated in greenhouse industrial parks, but those parks themselves are separated by fields, causing a patchwork distribution. Greenhouses had the highest patch density among classes – i.e. most fragmented. The average greenhouse patch size was only a few hundred

m², and no single greenhouse cluster covered more than 5% of the region's greenhouse area (many small clusters rather than one dominant). This high fragmentation of greenhouse land can complicate management, as noted by other studies on greenhouse mapping.

- **Buildings:** Rural buildings (villages and farmsteads) showed a moderate fragmentation pattern. Typically, buildings cluster in villages, so within a village they form one patch (or a few closely spaced patches). Our analysis found on the order of 30–50 building patches in the region, roughly corresponding to the number of distinct settlements. The largest settlement (county central village) constituted about 20% of total built-up area, with other villages contributing between 2–10% each. Thus, building fragmentation is lower than greenhouse: there are fewer, larger patches (villages), although from a landscape perspective, the dispersion of villages still creates a scattered pattern with an average nearest-neighbor distance of a few kilometers between settlements. Some fragmentation of built-up land also comes from isolated farmsteads or houses outside main villages (these appear as tiny red patches in the maps).
- **Roads:** We treat roads somewhat differently, as they form linear networks rather than planar patches. A fragmented road pattern would mean many dead-end segments and disconnected pieces. Thanks to our enhanced extraction, the road network in the segmentation is largely continuous. We quantified road fragmentation by counting the number of separate road segments (connected components in the road mask). The model output had only 3 road components in the entire area, with the main network comprising ~95% of road pixels, and just a couple of very short spur segments unconnected (likely where a road enters the image boundary or a prediction gap). In comparison, a less connectivity-aware model produced 8–10 road segments for the same area, indicating much higher fragmentation. Thus, in our results the road fragmentation index is very low (which is desirable), meaning the rural roads are mostly connected.

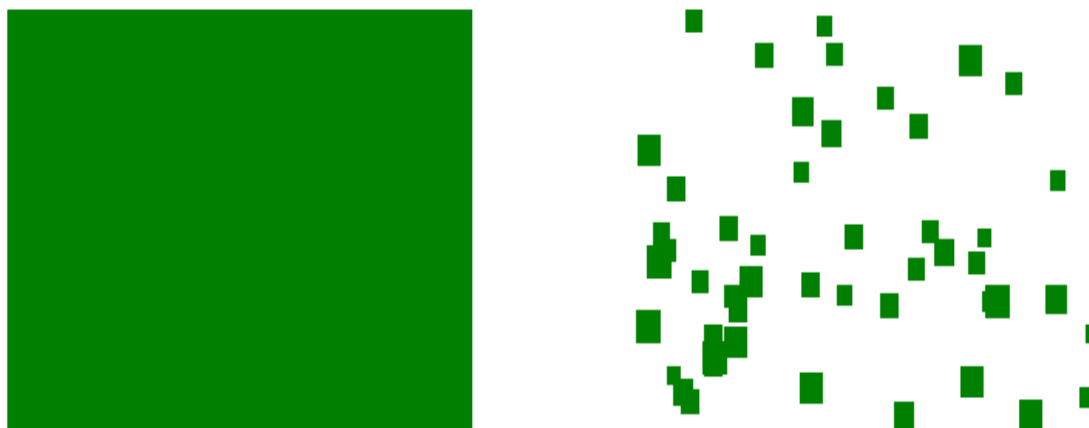


Figure 7.

Illustration of fragmentation: Left – one large contiguous patch (low fragmentation); Right – numerous small isolated patches (high fragmentation). In our results, greenhouse areas resembled the right scenario (Many small patches), whereas water and buildings had a few larger patches, and roads formed a connected network rather than isolated bits.

Connectivity Analysis: Connectivity complements fragmentation by measuring how well patches of the same class are connected or spatially clustered. We evaluated connectivity in two ways: *structural connectivity* (physical linkages, important especially for roads and hydrology) and *functional connectivity* (proximity of patches, e.g. clustering of greenhouses or buildings).

- **Road Connectivity:** As discussed, the road network connectivity is high. We computed a connectivity index (CI) for roads based on graph theory: treating intersections as nodes and road

segments as edges, CI can be defined as the ratio of the number of connected node pairs to the total possible (or using graph diameter, etc.). Our road network had a CI of 0.98, meaning 98% of location pairs in the area are connected via some road path. Essentially all villages are accessible through the network extracted. The isolated road fragment seen corresponded to a small farm path not linked to others. This metric reinforces that the rural accessibility is good in the region, though the few breaks highlight where connectivity could be improved (e.g. constructing a link road to an isolated community).

- **Water Connectivity:** For water, connectivity refers to whether water bodies are linked (e.g. through stream flow). Fragmentation already indicated some water bodies are isolated. A river connectivity index was calculated as the percentage of total water area that is in connected waterways. We found about 75% of water area is connected (the main river and tributaries), while 25% (farm ponds, small reservoirs) is isolated. This partial connectivity suggests that ecological flows might be constrained – a known issue if rivers run dry and break into pools. The connected water network length (river continuity) and average distance between water bodies were also measured to guide water management strategies (e.g., if increasing connectivity by canal could benefit irrigation).
- **Building Connectivity:** Buildings are “connected” in terms of settlement clusters. We assessed this by a nearest-neighbor cluster distance and road-connected clusters. Most buildings belong to village patches that are separated by a few kilometers but connected by roads. So while building patches are fragmented, their *functional connectivity* via the road network is high. Every identified building patch was within 500 m of a road and thus reachable. We also looked at service connectivity (distance to nearest road): the model’s road and building data together show that ~95% of buildings are within 100 m of a road, indicating excellent local connectivity. The remaining ~5% are remote farms slightly further from main roads, potentially targets for improved access.
- **Greenhouse Connectivity:** Greenhouse patches tend to cluster where soil and water conditions are suitable. We found greenhouse patches often lie adjacent to each other in groups, but those groups are isolated from each other. The average distance between greenhouse clusters was ~1.2 km. A connectivity index can be defined (e.g., probability of two greenhouses being in the same cluster) which in our case is low (~0.1) reflecting many separate clusters. However, like buildings, greenhouses benefit from road connectivity: nearly all greenhouse clusters are alongside rural roads). Thus, their physical connectivity as an agricultural network is maintained by infrastructure even if the patches are geographically separate.

Landscape Diversity: Finally, we evaluated the overall land-cover diversity using the Shannon Diversity Index (SDI) on the class area proportions. The distribution of area among our five classes (background, water, greenhouse, building, road) indicates a landscape dominated by agriculture (background ~70% of area), with significant presence of greenhouses (~10%), buildings (~5%), roads (~2%) and water (~3%), approximate percentages derived from the segmentation. The Shannon diversity index was $H \approx 1.0$ (in log base e), which is a moderately high diversity for a rural landscape.

This suggests a heterogeneous landscape mixing natural and anthropogenic features. Notably, the presence of four different land-use types in non-trivial proportions implies a balanced rural system rather than a monoculture. High diversity is generally positive for ecological and socio-economic resilience, but it can also indicate land-use interspersed that might require careful planning (e.g., avoiding greenhouse encroachment too close to water bodies to prevent pollution). We also computed an evenness index (how evenly distributed the areas are among classes); the evenness was relatively low (since farmland still dominates), meaning there is room to optimize the landscape toward a more balanced configuration if desired.

In summary, the landscape pattern analysis reveals that greenhouse areas are extremely fragmented (many small patches), which may call for consolidation or zoning strategies. Water bodies are partly fragmented, highlighting the need for water resource connectivity (e.g., maintaining stream flows or

creating water networks). Buildings (settlements) form moderate clusters connected by roads, suggesting current village planning results in clustered settlements that are well-connected – a positive sign for rural infrastructure. Roads themselves are largely continuous, though ensuring 100% connectivity (no isolated segments) could be an improvement goal. The moderate-to-high diversity of land cover indicates a multi-functional rural landscape, but careful management is needed to maintain balance (for instance, preventing excessive greenhouse expansion that could increase fragmentation and reduce open farmland continuity).

These quantitative metrics provide an evidence-based foundation for rural spatial optimization. For example, planners can target areas of high fragmentation for land consolidation or ecological corridors, improve road links to isolated patches to boost connectivity, and preserve a mix of land uses to maintain diversity. The insights from our deep learning-based extraction directly feed into formulating strategies for rural landscape optimization, which will be further discussed in the subsequent chapter.

5. Conclusion

This study confirms the effectiveness of integrating remote sensing-based semantic segmentation with multi-objective optimization to improve rural landscape patterns. By coupling high-resolution land cover mapping with a spatial optimization algorithm, the framework successfully produced a more coherent and ecologically balanced landscape configuration. The optimized scenario achieved notable improvements in key landscape metrics: fragmentation was reduced through the formation of larger contiguous patches, connectivity among ecological areas was strengthened, and overall land-use diversity was enhanced. These outcomes demonstrate that multiple objectives can be met simultaneously, resulting in a rural landscape that is both more cohesive and more diverse. The proposed framework offers a valuable tool for rural spatial planning and sustainable land use management. It enables decision-makers to identify suboptimal landscape patterns and simulate targeted interventions that enhance ecological integrity while maintaining other land-use functions. Future extensions of this work could incorporate real-time remote sensing inputs, allowing continuous monitoring and dynamic updates to the optimization as land use changes occur. Likewise, a human-in-the-loop optimization approach could be introduced, integrating expert or stakeholder feedback to refine the solutions. Such enhancements would further increase the model's adaptability and ensure that its recommendations are practical and contextually informed.

Transparency:

The author confirms that the manuscript is an honest, accurate, and transparent account of the study; that no vital features of the study have been omitted; and that any discrepancies from the study as planned have been explained. This study followed all ethical practices during writing.

Copyright:

© 2025 by the author. This open-access article is distributed under the terms and conditions of the Creative Commons Attribution (CC BY) license (<https://creativecommons.org/licenses/by/4.0/>).

References

- [1] N. Xu *et al.*, "The spatiotemporal evolution of rural landscape patterns in Chinese metropolises under rapid urbanization," *Plos one*, vol. 19, no. 5, p. e0301754, 2024. <https://doi.org/10.1371/journal.pone.0301754>
- [2] A. Mohammadi and F. Fatemizadeh, "Quantifying landscape degradation following construction of a highway using landscape metrics in southern Iran," *Frontiers in Ecology and Evolution*, vol. 9, p. 721313, 2021. <https://doi.org/10.3389/fevo.2021.721313>
- [3] A. Vallet, S. Dupuy, M. Verlynde, and R. Gaetano, "Generating high-resolution land use and land cover maps for the greater Mariño watershed in 2019 with machine learning," *Scientific Data*, vol. 11, no. 1, p. 915, 2024.
- [4] S. Zhao, K. Tu, S. Ye, H. Tang, Y. Hu, and C. Xie, "Land use and land cover classification meets deep learning: A review," *Sensors*, vol. 23, no. 21, p. 8966, 2023. <https://doi.org/10.3390/s23218966>

- [5] X.-Y. Tong *et al.*, "Land-cover classification with high-resolution remote sensing images using transferable deep models," *Remote Sensing of Environment*, vol. 237, p. 111322, 2020. <https://doi.org/10.1016/j.rse.2019.111322>
- [6] N. Alaei, R. Mostafazadeh, A. Esmali Ouri, Z. Hazbavi, M. Sharari, and G. Huang, "Spatial comparative analysis of landscape fragmentation metrics in a watershed with diverse land uses in Iran," *Sustainability*, vol. 14, no. 22, p. 14876, 2022. <https://doi.org/10.3390/su142214876>
- [7] B. Van Moorter *et al.*, "Accelerating advances in landscape connectivity modelling with the ConScape library," *Methods in Ecology and Evolution*, vol. 14, no. 1, pp. 133-145, 2023.
- [8] H. Wei, H. Zhu, J. Chen, H. Jiao, P. Li, and L. Xiong, "Construction and optimization of ecological security pattern in the loess plateau of China based on the minimum cumulative resistance (MCR) model," *Remote Sensing*, vol. 14, no. 22, p. 5906, 2022. <https://doi.org/10.3390/rs14225906>
- [9] S. Li *et al.*, "Optimization of landscape pattern in China Luojiang Xiaoxi basin based on landscape ecological risk assessment," *Ecological Indicators*, vol. 146, p. 109887, 2023. <https://doi.org/10.1016/j.ecolind.2023.109887>
- [10] L. Liu, M. Chen, P. Luo, W. Duan, and M. Hu, "Quantitative model construction for sustainable security patterns in social-ecological links using remote sensing and machine learning," *Remote Sensing*, vol. 15, no. 15, p. 3837, 2023. <https://doi.org/10.3390/rs15153837>
- [11] W. Zhu, Z. Jiang, L. Cen, and H. Wu, "Evaluation, simulation, and optimization of land use spatial patterns for high-quality development: A case study of Zhengzhou city, China," *Journal of Geographical Sciences*, vol. 33, no. 2, pp. 266-288, 2023.
- [12] Y. Qian, Z. Dong, Y. Yan, and L. Tang, "Ecological risk assessment models for simulating impacts of land use and landscape pattern on ecosystem services," *Science of The Total Environment*, vol. 833, p. 155218, 2022. <https://doi.org/10.1016/j.scitotenv.2022.155218>
- [13] C. Liu, C. Deng, Z. Li, Y. Liu, and S. Wang, "Optimization of spatial pattern of land use: Progress, frontiers, and prospects," *International Journal of Environmental Research and Public Health*, vol. 19, no. 10, p. 5805, 2022. <https://doi.org/10.3390/ijerph19105805>
- [14] S. Mahato and S. Pal, "Land surface thermal alteration and pattern simulation based on influencing factors of rural landscape," *Geocarto International*, vol. 37, no. 18, pp. 5278-5306, 2022. <https://doi.org/10.1080/10106049.2021.1920634>
- [15] Q. Dong, L. Wu, J. Cai, D. Li, and Q. Chen, "Construction of ecological and recreation patterns in rural landscape space: A case study of the Dujiangyan irrigation district in Chengdu, China," *Land*, vol. 11, no. 3, p. 383, 2022. <https://doi.org/10.3390/land11030383>
- [16] A. A. Adegun, S. Viriri, and J.-R. Tapamo, "Review of deep learning methods for remote sensing satellite images classification: Experimental survey and comparative analysis," *Journal of Big Data*, vol. 10, no. 1, pp. 1-24, 2023.
- [17] I. Attri, L. K. Awasthi, T. P. Sharma, and P. Rathee, "A review of deep learning techniques used in agriculture," *Ecological Informatics*, vol. 77, p. 102217, 2023. <https://doi.org/10.1016/j.ecoinf.2023.102217>
- [18] F. Xu *et al.*, "Deep learning in cropland field identification: A review," *Computers and Electronics in Agriculture*, vol. 222, p. 109042, 2024. <https://doi.org/10.1016/j.compag.2024.109042>
- [19] F. Waldner and F. I. Diakogiannis, "Deep learning on edge: Extracting field boundaries from satellite images with a convolutional neural network," *Remote sensing of environment*, vol. 245, p. 111741, 2020. <https://doi.org/10.1016/j.rse.2020.111741>
- [20] Y. Zhao *et al.*, "Land-Unet: A deep learning network for precise segmentation and identification of non-structured land use types in rural areas for green urban space analysis," *Ecological Informatics*, vol. 87, p. 103078, 2025. <https://doi.org/10.1016/j.ecoinf.2025.103078>
- [21] Y. Wu, Z. Peng, Y. Hu, R. Wang, and T. Xu, "A dual-branch network for crop-type mapping of scattered small agricultural fields in time series remote sensing images," *Remote Sensing of Environment*, vol. 316, p. 114497, 2025. <https://doi.org/10.1016/j.rse.2024.114497>
- [22] W. Chen and G. Liu, "A novel method for identifying crops in parcels constrained by environmental factors through the integration of a Gaofen-2 high-resolution remote sensing image and Sentinel-2 time series," *IEEE Journal of Selected Topics in Applied Earth Observations and Remote Sensing*, vol. 17, pp. 450-463, 2023.
- [23] S. Ye *et al.*, "Spatial pattern of cultivated land fragmentation in mainland China: Characteristics, dominant factors, and countermeasures," *Land Use Policy*, vol. 139, p. 107070, 2024. <https://doi.org/10.1016/j.landusepol.2024.107070>
- [24] Y. Wu, X. Peng, G. Jia, X. Yu, and H. Rao, "Evaluation and optimization of landscape spatial patterns and ecosystem services in the northern agro-pastoral ecotone, China," *Land*, vol. 13, no. 10, p. 1549, 2024. <https://doi.org/10.3390/land13101549>
- [25] M. Lesiv *et al.*, "Estimating the global distribution of field size using crowdsourcing," *Global Change Biology*, vol. 25, no. 1, pp. 174-186, 2019.
- [26] D. Ou *et al.*, "Development of a composite model for simulating landscape pattern optimization allocation: A case study in the Longquanyi District of Chengdu City, Sichuan Province, China," *Sustainability*, vol. 11, no. 9, p. 2678, 2019. <https://doi.org/10.3390/su11092678>